Front. Optoelectron. 2013, 6(4): 440–447
DOI 10.1007/s12200-013-0350-x

RESEARCH ARTICLE

Selective growth and characterization of ZnO nanorods assembled a hexagonal pattern on H_2-decomposed GaN epilayer

Yu TIAN[1,2], Huiquan CHEN[2], Xiaolong ZHU (✉)[1], Guang ZHENG[1], Jiangnan DAI[2]

1 Department of Physics, Jianghan University, Wuhan 430056, China
2 Wuhan National Laboratory for Optoelectronics, Huazhong University of Science and Technology, Wuhan 430074, China

Abstract This paper reported a simple and effective method for fabricating and patterning highly ordered ZnO nanorod arrays on H_2-decomposed GaN epilayer via hydrothermal route. The edge of pattern, which has been decomposed by H_2 flow, provides appropriate nucleation sites for the selective-growth of aligned ZnO nanorods. The density of ZnO nanorod arrays assembled the hexagonal pattern can be tuned by varying the solution concentrations, growth time and reaction temperatures. The results have demonstrated that the ZnO nanorods are highly uniform in diameter and height with perfect alignment and are epitaxially grown along [0001] direction. This work provides a novel and accessible route to prepare oriented and aligned ZnO nanorod arrays pattern. And the aligned ZnO nanorods form an ideal hexagonal pattern that might be used in many potential applications of ZnO nanomaterials.

Keywords ZnO nanorod, GaN epilayer, hexagonal pattern, hydrothermal

1 Introduction

One-dimensional (1D) semiconducting nanostructures have been extensively studied due to their potential applications in nanoelectronic devices. Wurtzite zinc oxide (ZnO) is considered the most promising material for short wavelength optoelectronic devices because of its direct wide bandgap energy of 3.37 eV, and a large exciton binding energy of 60 meV at room temperature. ZnO 1D nanostructures, such as nanowires, nanorods and nanotubes, have attracted extensive attention over the past few years, because of their unique electrical and optical properties [1–3]. In particular, patterned and aligned 1D ZnO nanostructure arrays, which can bring improved optoelectronic performance, are the most attractive [4]. Dimension adjustable, highly oriented, periodic ZnO nanorod/nanowire arrays are highly desirable for the realization of advanced photonic optical devices [5]. Traditionally, the fabrication of patterned and aligned 1D ZnO nanostructure arrays can be achieved via vapor-liquid-solid (VLS) growth on the patterned catalyst/seed sites created by electron-beam lithography (EBL) [6], laser interference lithography (LIL) [7], nanoimprint lithography (NIL) [8] or self-assembled nanosphere lithography (NSL) [9,10]. However, the temperature for VLS method is too high for direct application on various substrates. Furthermore, it may also have a risk of introducing catalyst residual atoms into ZnO. Usually, the resulting ZnO nanostructures are distributed randomly or poor crystallization [11,12], which largely limits their application in high performance optoelectronic devices. Compared with the conventional VLS method, hydrothermal growth shows some advantages, such as the use of simple equipment, low-temperature deposition (about 100°C), low cost, less hazard, and no need for the use of metal catalysts.

Here, Gallium nitride (GaN) film was used as a template for the ZnO nanorod growth since these materials have the same wurtzite crystal structure, low lattice constant misfit (1.9%) and similar thermal expansion. There have been many examples of catalyst-free epitaxial growth of ZnO nanowires on GaN using metal-organic chemical vapor deposition (MOCVD) [13,14] or from aqueous solutions [15–22] but no clear explanation for 1D growth. In fact, the favorable lattice match between the basal planes of GaN and ZnO [23] would tend to promote two-dimensional

Received May 29, 2013; accepted July 1, 2013

E-mail: xlzhu.jhun@gmail.com

(2D) epitaxial film growth over 1D nanowire growth. It was realized that GaN substrates were so effective at enabling epitaxial 1D growth of ZnO nanowires/nanorods. Probably because GaN thin film grown on sapphire substrate contain high densities of dislocations [24], and these dislocations at can actually act as growth site to assist dislocation-driven 1D growth [25].

In this paper, a facile and effective approach to the selective-growth of highly ordered and vertically aligned ZnO nanorod arrays on the H_2-decomposed GaN/sapphire substrate via a hydrothermal route is reported. For the preparation of the patterned GaN substrate, H_2 was used to decompose the GaN epilayer grown by MOCVD, and some hexagonal patterns were obtained on the GaN epilayer, then the patterned GaN epilayer were used to propagate the growth of epitaxial ZnO nanorods directly from aqueous solutions. ZnO nanorod arrays grow from the GaN epilayer, and the coalescence of multiple ZnO nanorods to a thicker nanorod from single growth site can be realized at the appropriate solution concentration, growth time and reaction temperature. The ordered ZnO nanorods are highly uniform in diameter and height with perfect alignment and are epitaxially grown along [0001] direction. And the growth mechanism will also be discussed in detail.

2 Experimental methods

The GaN epilayer was prepared by growing an 800 nm GaN film on *c*-plane sapphire by a horizontal-type low-pressure (~40 Torr) MOCVD system. The triethyleneglycol (TEG), trimethylaluminium (TMAl) and ammonia were used as source gas for Ga, Al and N, respectively. Hydrogen was used as the carrier gas. First a thin AlN nucleation layer was deposited directly on the *c*-plane sapphire at the temperature of 620°C, then a high temperature using AlN buffer pulsed atomic layer epitaxy (PALE) method was deposited on the low temperature nucleation layer at the temperature of 1050°C. At last GaN epilayer about 800 nm thick was grown on the PALE-AlN buffer at the temperature of 940°C. Then GaN decomposition occurred by flowing pure H_2 at 1050°C for 5 min, and GaN epilayer with hexagonal patterns will be obtained.

Reagent grade zinc nitrate hexahydrate (ZNH) and hexam-ethylenetetramine (HMT) were used for the synthesis of patterned ZnO nanorod arrays. Aqueous solution of ZNH and HMT was prepared using deionized water with equal concentrations (0.05 mol/L) for the growth of nanorods. The *c*-plane GaN/sapphire substrate was subjected to sequential ultrasonic rinsing in acetone, ethanol and deionized water prior to inserting in growth solution. The substrate was then placed in a Teflon liner containing 80 mL precursor solution, with the GaN template layer facing downwards on a special glass instrument. The Teflon container was tightly closed in a stainless steel autoclave. The autoclave was placed in an oven for a period of 2 h at a temperature of 105°C. On completion of reaction, the container was cooled naturally to room temperature. The sample was taken out, washed in deionized water several times and dried in air.

The resulting ZnO nanorods on GaN were characterized by field emission scanning electron microscopy (JEOL 6700FESEM). The crystalline and microstructure properties were analyzed by using X-ray diffraction (XRD: PhilipsX'Pert) and transmission electron microscopy (TEM: Philips CM300) respectively. The photoluminescence (PL) measurement was carried out to characterize the optical property of the ZnO nanorods using a 325 nm He-Cd laser as the excited source.

3 Results and discussion

Figure 1 shows the morphological images of ZnO nanorods on H_2-decomposed GaN epilayer. Some hexagonal patterns assembled with vertical epitaxial ZnO nanorods have been observed over a large area, which are consistent with the hexagonal crystal structure of ZnO. At the same time, additional hexagonal ZnO nanorods were also present. The micrographs of the ZnO nanorods were observed at 1000×(Fig. 1(a)), 8000×(Figs. 1(b) and 1(c)), 15000×(Fig. 1(d)), and 60000×(Fig. 1(e)) magnifications, respectively. From the micrographs, ZnO nanorod was inclined to grow at edge of the large hexagonal pits resulting to a hexagonal pattern, shown in Figs. 1(b) and 1 (c). And the sizes of hexagonal patterns are similar as the hexagonal pits. When there were no evident hexagonal pits, ZnO nanorod was still distributed perpendicular to the GaN epilayer surface but no with regular distribution (Figs. 1(d) and 1(e)). The length and diameter of the ZnO nanorods were measured at about 3 μm and 500 nm, respectively. In our experiments, the diameter, length and density of the ZnO nanorods can be changed by varying the reactant concentration, growth time and temperature. If high inerratic hexagonal pits fabricating on GaN epilayer by H_2-decomposed, the vertical epitaxial ZnO nanorods which assembled regularly for hexagonal patterns will be obtained. Therefore fabricating nanostructures in a controllable way, it is critical to fabricate a high quality mask with dimensions at the nano scale.

The X-ray diffraction (XRD) measurement was carried out to characterize the crystal structure of the ZnO nanorods, as shown in Fig. 2(a). The strong ZnO (002) diffraction peak was consistent with the SEM images, which demonstrate the oriented arrays of ZnO nanorods assembled the hexagonal pattern with a preferential growth in the *c*-axis direction. The observed ZnO (002) diffraction peak was indexed to the hexagonal phase of ZnO. The crystallinity and texture of H_2-decomposed GaN epilayer were significant for the subsequent growth of ZnO

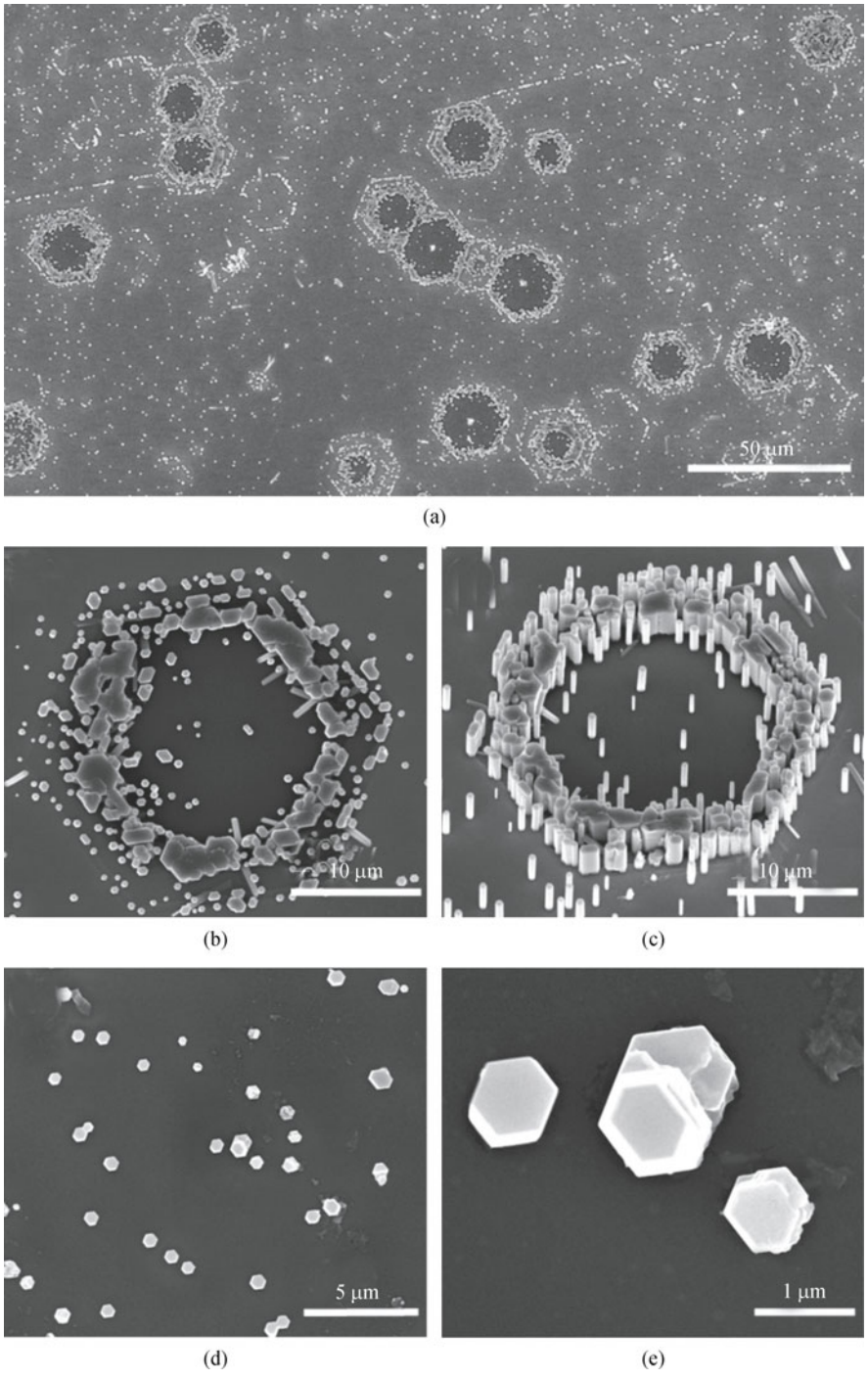

Fig. 1 (a) Top-view of the patterned and aligned ZnO nanorod arrays on the H_2-decomposed GaN epilayer grown by hydrothermal reaction; (b, c) top-view and 30° tilt view nanorods assembled a hexagonal pattern; (d, e) other nanorods distributed perpendicular to the GaN epilayer surface without regular distribution

nanorods, especially the edge of GaN hexagonal pattern. A typical HRTEM image of an individual nanorod (the inserted TEM image) grown on the GaN epilayer is described in Fig. 2(b). It clearly shows that the ZnO nanorod possesses a single-crystal structure. Furthermore, the spacing of 0.26 nm between adjacent lattice planes corresponds to the distance of (0002) planes, showing that [0001] is the growth direction of the ZnO nanorods.

To investigate the growth process of ZnO nanorod assembled a hexagonal pattern; hydrothermal growths at different solution concentration, growth time and reaction temperature were also performed. When synthesizing at lower solution concentration of 0.002 and 0.01 mol/L, sparse and thin nanorods had obtained at the edge of

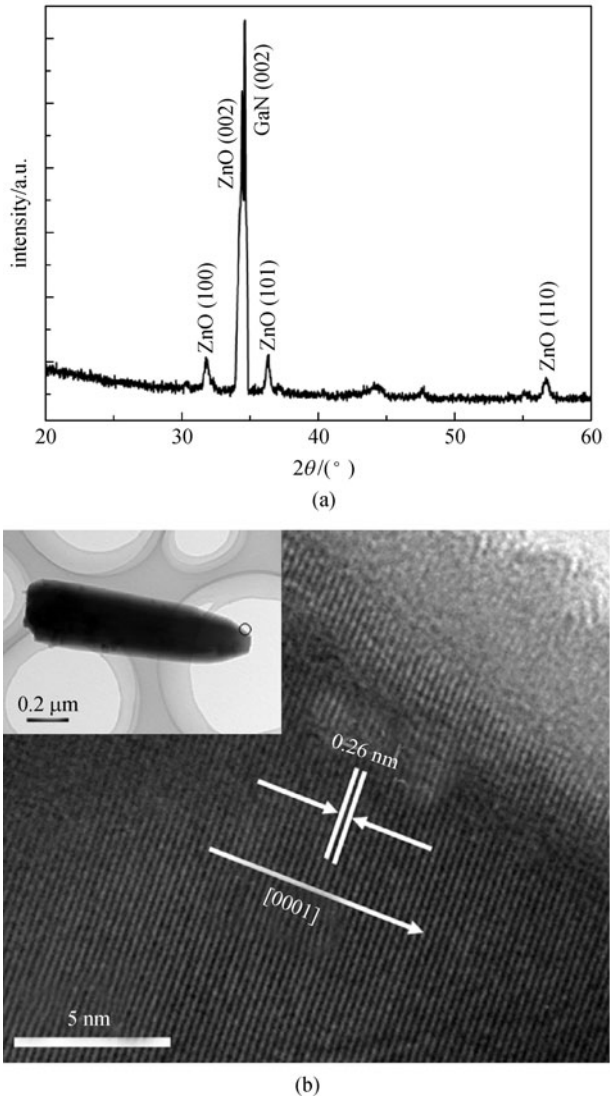

Fig. 2 (a) XRD pattern of ZnO nanorod arrays on the H_2-decomposed GaN epilayer; (b) HRTEM image of a single ZnO nanorod confirming growth along the [0001] direction, inset is a low-resolution bright-field TEM image of the corresponding single ZnO nanorod where the area of analysis is indicated by the black circle

hexagonal etch pits, as shown in Figs. 3(A_1) and 3(A_2). The size of the hexagonal patterns was on the scale of micrometers and each hexagonal pattern consisted of aggregates of nanorods with sizes of 150 – 300 nm. In this case, ZnO nanorods become gradually dense and thick with increasing solution concentration. It is interrelated to increasing nucleation at the edge of hexagonal etch pits on the GaN epilayer. By increasing growth time to 4 or 7 h and keeping other conditions under the same, those ZnO nanorods assembled the hexagonal pattern have been merged into thicker nanorods (Fig. 3(B_1)). Especially, when growth time keep for 7 h, it is obvious that the hexagonal pattern has been assembled with connected nanorods, as shown in Fig. 3(B_2). If there are two or more steps in the H_2-decomposed GaN hexagonal pits, ZnO nanorods will formed series of hexagonal pattern (shown in Fig. 3(B_1)). The nanorods have no evident change where sparsely distributed other places, such as near the hexagonal pattern. When altering reaction temperature to 125°C, the ZnO nanorods almost integrate to form a hexagonal pattern; and a diverting phenomenon occurred: some nanotubes are present among the nanorods and some nanorods become broken, as shown in Fig. 3(C_1). With reaction temperature increasing to 160°C, there are no nanorods formed only leaving a H_2-decomposed GaN hexagonal pattern (Fig. 3(C_2)). From these results, the experimental conditions could tune the density or dimension of ZnO nanorods. And these experimental conditions have been listed in Table 1. Furthermore, if we employ GaN substrates that have not been decomposed by H_2, only a few ZnO nanorods were obtained randomly on the GaN substrates, visible under SEM (Figs. 3 (D_1) and 3(D_2)).

The observation of experiments about these epitaxial ZnO nanorods and on the H_2-decomposed GaN substrates supports our hypothesis that two main growth steps may occur in the synthetic process. First, some selective growth sites for ZnO nanorods growth were present on the GaN epilayer. In our experiment, GaN film was decomposed by flowing pure H_2 at 1050°C for 5 min resulting in some hexagonal pits and many small dislocations, as shown in Fig. 4(b). Secondly, ZnO nanorods grow from these growth sites and then formed the hexagonal patterns or scattered nanorods. In this stage, the ZnO nanorods grow via edge effect and a dislocation-driven mechanism [25]. On one side, H_2-etched hexagonal pattern provided some selective growth sites for ZnO nanorods, especially the edge of hexagonal pattern. These edges were prone for ZnO nanorod growth because of low energy and shape variation. So it is mainly edge effect controlling the ZnO nanorods growth assembled the hexagonal pattern (shown in Fig. 4(c)). On the other hand, small dislocations were another growth sites for ZnO nanorods growth which are distributed perpendicular to the GaN epilayer surface but no with regular distribution, as shown in Figs. 1(d) and 1(e). It is similar to the result which has been reported by Morin and Jin [25]. It is apparent that every ZnO nanorod grown originates from a dislocation etch pit. We speculate this is where the dislocation etch pits were “filled in” during the initial stages of nanorod growth. With reaction time increasing, ZnO nanorods gradually grow to become long and thick on the initial sites. Due to close lattice matching between ZnO and GaN, heterogeneous nucleation has lower activation energy barrier than homogeneous nucleation. It is also known that different faces of ZnO crystal exhibit disproportionate growth rates. The (0001) face of ZnO grows much faster compared to other faces [26,27]. Therefore, upon nucleation, ZnO grows along the [0001] direction faster than other directions resulting in the nanorod morphology and ZnO nanorod are distributed perpendicular to the surface of GaN epilayer. The

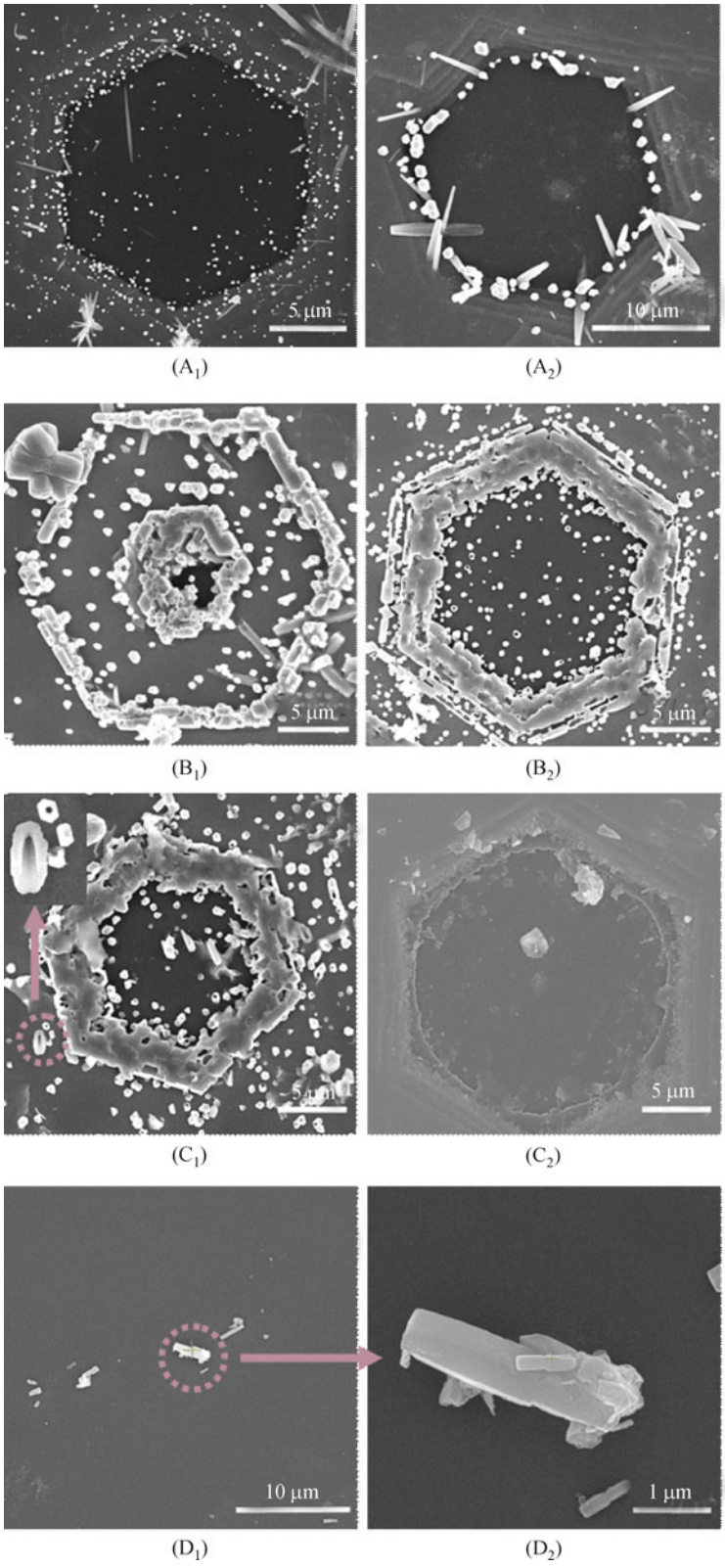

Fig. 3 Patterned ZnO nanorod arrays on H_2-decomposed GaN epilayer growing at different solution concentrations, growth times and reaction temperatures. (A_1, A_2) 0.002 and 0.01 mol/L, 105°C for 2 h; (B_1, B_2) 4 and 7 h, 0.05 mol/L for 105°C; (C_1, C_2) 125 and 160°C, 0.05 mol/L for 4 h; (D_1, D_2) SEM images of ZnO nanorod growing on GaN epilayer without decomposition

Table 1 Experimental conditions of ZnO nanorod growing at different solution concentration, growth time and reaction temperature

samples	concentration/(mol·L^{-1})	growth time/h	temperature/°C
A_1	0.002	2	105
A_2	0.01	2	105
B_1	0.05	4	105
B_2	0.05	7	105
C_1	0.05	4	125
C_2	0.05	4	160

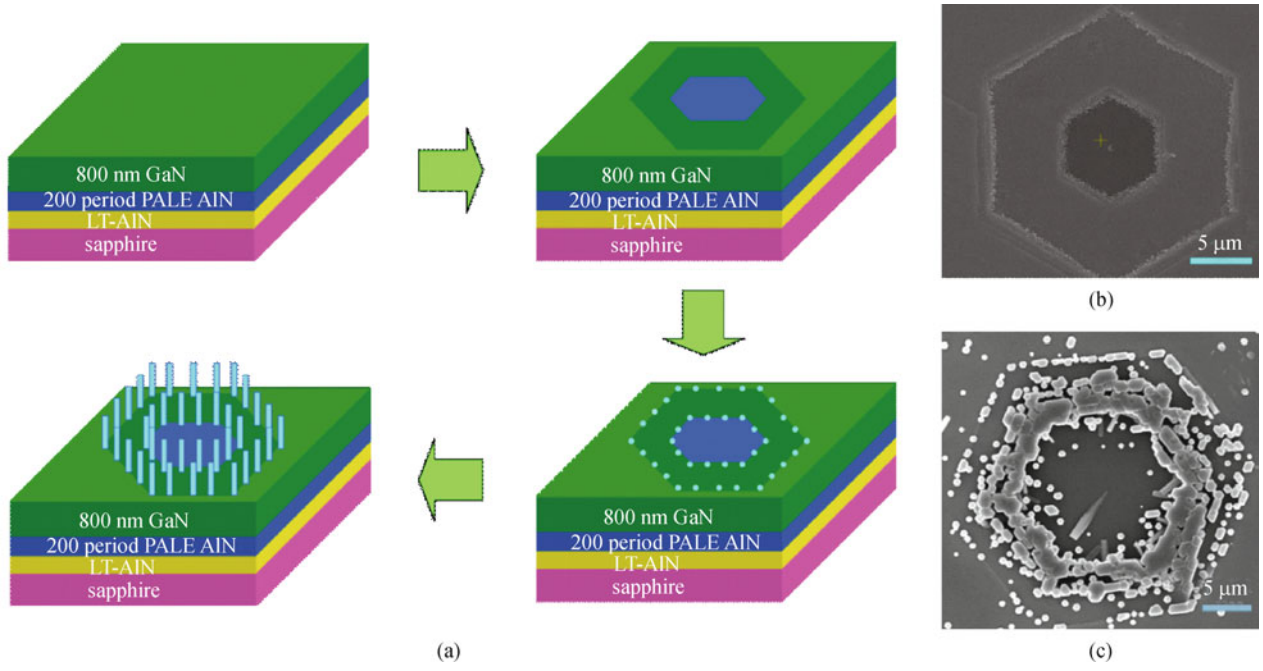

Fig. 4 (a) Schematic of fabrication of patterned ZnO nanorod arrays pattern on H_2-decomposed GaN epilayer; (b) SEM image of a hexagonal pattern has been obtained by H_2 decomposed; (c) SEM image of ZnO nanorod arrays grown at the edge of the hexagonal pattern

schematic of fabrication of patterned ZnO nanorod arrays pattern on H_2-decomposed GaN epilayer was shown in Fig. 4(a).

By altering experimental conditions, the results reveal that the concentration of ZNH/HMT and growth time play important roles in controlling the density of the ZnO nanorods. A relation to the density of the initial seeding was found that at the edge of hexagonal pattern the nanorods grow much more vertically aligned than those growing at small dislocation etch pits. By the adjustment of the growth time the nanorods incorporate one or more thick rods, it is interrelated to dense growth sites formation at the edge of hexagonal pattern. So the larger the relative amount of zinc nitrate and the longer growth time, the denser is the initial seeding and final nanorods. While by the adjustment of the growth temperature, there are some broken nanorods assembled the hexagonal pattern and some nanotubes are also present. It is probable that a high reaction temperature is a disadvantage for the nanorods growth. Especially, when reaction temperature increases to 160°C, there are no nanorods formed, only leave a H_2-decomposed GaN hexagonal pattern. It is possible that reaction temperature is too high to nucleate on the GaN epilayer.

As a potential photonic material, it is important to evaluate the optical properties of ZnO nanorods. Photoluminescence (PL) measurement was performed on the ZnO nanorod/GaN epilayer, since it was an effective method for investigating the presence of defects. The PL spectrum measured at room temperature from the as-grown ZnO nanorod arrays is shown in Fig. 5(a). It shows a strong UV emission centered at 383 nm and a weak and broad green emission centered at 518 nm. The UV emission is usually considered as the characteristic emission of ZnO, and the UV emission peak usually originates from the near band-edge emission from the recombination of free excitons [28]. Generally speaking, the green emission centered at 518 nm is attributed to the singly ionized oxygen vacancy in ZnO and the emission results from the radiative recombination of a photon-generated hole with an electron occupying the oxygen vacancy [29,30]. However, Zeng et al. deliberated that the violet and blue emissions

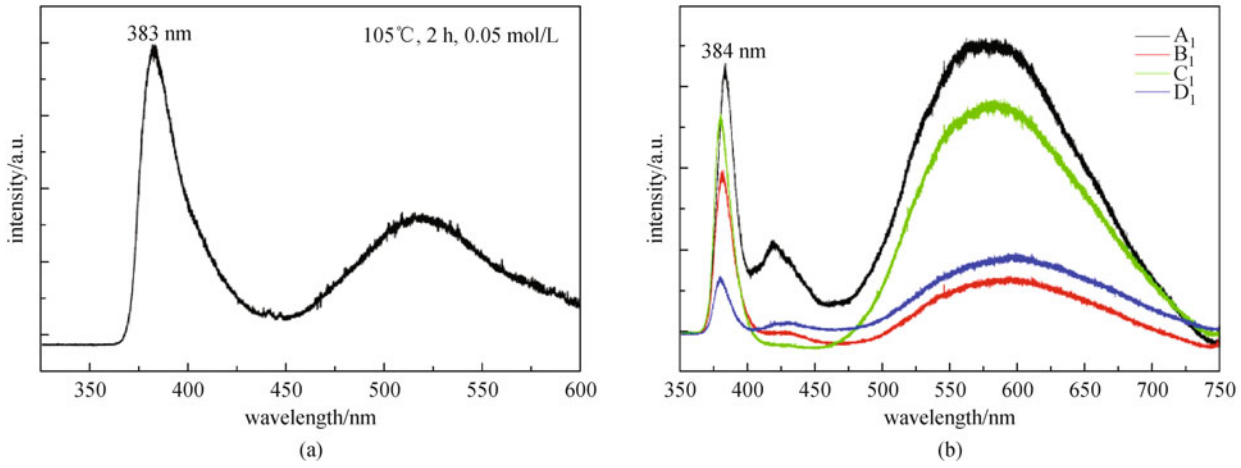

Fig. 5 (a) PL spectrum of patterned ZnO nanorod arrays grow on H_2-decomposed GaN epilayer; (b) PL spectra of other samples grown on different experiments

are attributed to the transitions from Zn_i and extended Zn_i states to the valance band, respectively [31]. In our work, the intensity ratio of the UV emission and the visible emission of the ZnO products with the reaction time of 2 h is 4.93, indicating that the visible emission is not negligible compared with the relatively intense UV emission. According to the Zeng's report, we think the UV emission complies with their excitation modes. For the violet emission, if the electrons are excited up to a sub-band of the conduction band, they can first relax to Zn_i state through a nonradiative transition, and then transit to the valance band. So the excitation mode, with $E_g \leqslant E_{ex}$, is effective for violet emissions. Blue emissions can be attributed to the transition from extended Zn_i states, which are slightly below the simple Zn_i state, to the valance band.

And the PL spectra of other samples were measured, too. From Fig. 5(b), the samples of A_1, B_1, C_1 and D_1 were displayed. In these samples, the sample D_1 is ZnO nanorod growing on GaN epilayer without decomposition. Its PL spectrum shows that the intensity of UV emission is lower than that of the green emission. So it implies that the crystal of ZnO nanorod is poor. And the PL spectra of other samples show the crystal of ZnO nanorod becomes poor when decreasing concentration or rising temperature. In these spectra of the samples, the PL spectrum of B_1 sample is similar with that of the patterned ZnO nanorod arrays suggesting the crystal of ZnO nanorods in between two samples is akin. To the PL spectrum of A_1, there is a small peak centered at 419 nm. According to the mechanism of Zeng's report, two excitation modes, with $E_g \leqslant E_{ex}$ and $E_{Zn_i} \leqslant E_{ex} < E_g$, are effective for violet emissions. So the blue emissions of these samples can be attributed to the transition from extended Zn_i states, which are slightly below the simple Zn_i state, to the valance band. For the D_1 sample possessing out-of-order ZnO nanorods, because of the fewer amount ZnO nanorods, so the intensities of the UV emission and blue emissions could be relatively weaker. For the special optical properties of the patterned ZnO nanorod arrays because of highly oriented, dimension adjustable, they are highly desirable for the realization of advanced photonic optical devices.

4 Conclusions

In summary, we have developed an effective approach to the selective-growth of vertically aligned ZnO nanorod arrays assembled hexagonal patterns on the H_2-decomposed GaN epilayer via a hydrothermal route. Taking advantage of the edge of hexagonal pattern pits, the nanorods of ZnO can be easily grown from the edges assembled a hexagonal pattern. At the same time, the nanorods were also grown from the dislocation etch pits which had been obtained by H_2-decomposed on the GaN epilayer. These dislocations etch pits or the edges of hexagonal patterns offered selective growth sites for ZnO nanorods. The density and dimension of the ZnO nanorods can be tuned by solution concentration, growth time and reaction temperature. The ordered ZnO nanorods with perfect alignment are epitaxially grown along [0001] direction. The properties of these ZnO nanorods promise their potential applications in advanced photonic optical devices.

Acknowledgements This work was supported by the Starting Research Fund from the Jianghan University (Nos. 2010014 and 2012017), the National Natural Science Foundation of China (Grant Nos. 61006046 and 51002058).

References

1. Wang X D, Song J H, Liu J, Wang Z L. Direct-current nanogenerator

driven by ultrasonic waves. Science, 2007, 316(5821): 102–105
2. Lee S W, Jeong M C, Myoung J M, Chae G S, Chung I J. Magnetic alignment of ZnO nanowires for optoelectronic device applications. Applied Physics Letters, 2007, 90(13): 133115
3. Lee Y J, Ruby D S, Peters D W, McKenzie B B, Hsu J W P. ZnO nanostructures as efficient antireflection layers in solar cells. Nano Letters, 2008, 8(5): 1501–1505
4. Lin M S, Chen C C, Wang W C, Lin C F, Chang S Y. Fabrication of the selective-growth ZnO nanorods with a hole-array pattern on a p-type GaN:Mg layer through a chemical bath deposition process. Thin Solid Films, 2010, 518(24): 7398–7402
5. Xu S, Xu C, Liu Y, Hu Y F, Yang R S, Yang Q, Ryou J H, Kim H J, Lochner Z, Choi S, Dupuis R, Wang Z L. Ordered nanowire array blue/near-UV light emitting diodes. Advanced Materials, 2010, 22 (42): 4749–4753
6. Ng H T, Han J, Yamada T, Nguyen P, Chen Y P, Meyyappan M. Single crystal nanowire vertical surround-gate field-effect transistor. Nano Letters, 2004, 4(7): 1247–1252
7. Kim D S, Ji R, Fan H J, Bertram F, Scholz R, Dadgar A, Nielsch K, Krost A, Christen J, Gösele U, Zacharias M. Laser-interference lithography tailored for highly symmetrically arranged ZnO nanowire arrays. Small, 2007, 3(1): 76–80
8. Hochbaum A I, Fan R, He R, Yang P. Controlled growth of Si nanowire arrays for device integration. Nano Letters, 2005, 5(3): 457–460
9. Dong J J, Zhang X W, Yin Z G, Zhang S G, Wang J X, Tan H R, Gao Y, Si F T, Gao H L. Controllable growth of highly ordered ZnO nanorod arrays via inverted self-assembled monolayer template. Applied Materials & Interfaces, 2011, 3(11): 4388–4395
10. Fan H J, Fuhrmann B, Scholz R, Syrowatka F, Dadgar A, Krost A, Zacharias M. Well-ordered ZnO nanowire arrays on GaN substrate fabricated via nanosphere lithography. Journal of Crystal Growth, 2006, 287(1): 34–38
11. Zeng H B, Xu X J, Bando Y, Gautam U K, Zhai T Y, Fang X S, Liu B D, Golberg D. template deformation-tailored ZnO nanorod/ nanowire arrays: full growth control and optimization of field-emission. Advanced Functional Materials, 2009, 19(19): 3165–3172
12. Cheng C, Lei M, Feng L, Wong T L, Ho K M, Fung K K, Loy M M T, Yu D P, Wang N. High-quality ZnO nanowire arrays directly fabricated from photoresists. ACS Nano, 2009, 3(1): 53–58
13. Hong Y J, An S J, Jung H S, Lee C H, Yi G C. Position-controlled selective growth of ZnO nanorods on Si substrates using facet-controlled GaN micropatterns. Advanced Materials, 2007, 19(24): 4416–4419
14. Hong Y J, Yoo J, Doh Y J, Kang S H, Kong K J, Kim M, Lee D R, Oh K H, Yi G C J. Controlled epitaxial growth modes of ZnO nanostructures using different substrate crystal planes. Materials Chemistry, 2009, 19(7): 941–947
15. Le H Q, Chua S J, Koh Y W, Loh K P, Chen Z, Thompson C V, Fitzgerald E A. Growth of single crystal ZnO nanorods on GaN using an aqueous solution method. Applied Physics Letters, 2005, 87(10): 101908
16. Wei Y G, Wu W Z, Guo R, Yuan D J, Das S, Wang Z L. Wafer-scale high-throughput ordered growth of vertically aligned ZnO nanowire arrays. Nano Letters, 2010, 10(9): 3414–3419
17. Tay C B, Le H Q, Chua S J, Loh K P J. Empirical model for density and length prediction of ZnO nanorods on GaN using hydrothermal synthesis. Journal of the Electrochemical Society, 2007, 154(9): K45–K50
18. Le H Q, Chua S J, Koh Y W, Loh K P, Fitzgerald E A. Systematic studies of the epitaxial growth of single-crystal ZnO nanorods on GaN using hydrothermal synthesis. Journal of Crystal Growth, 2006, 293(1): 36–42
19. Gao H Y, Yan F W, Li J M, Zeng Y P, Wang J X. Synthesis and characterization of ZnO nanorods and nanoflowers grown on GaN-based LED epiwafer using a solution deposition method. Journal of Physics. D, Applied Physics, 2007, 40(12): 3654–3659
20. Zhou H L, Shao P G, Chua S J, Kan J A, Bettiol A A, Osipowicz T, Ooi K F, Goh G K L, Watt F. Selective growth of ZnO nanorod arrays on a GaN/sapphire substrate using a proton beam written mask. Crystal Growth & Design, 2008, 8(12): 4445–4448
21. Ye B U, Yu H, Kim M H, Lee J L, Baik J M. Modulating ZnO nanostructure arrays on any substrates by nanolevel structure control. Journal of Physical Chemistry C, 2011, 115(16): 7987–7992
22. Sun Y, Riley J, Ashfold M N R. Mechanism of ZnO nanotube growth by hydrothermal methods on ZnO film-coated Si substrates. Journal of Physical Chemistry B, 2006, 110(31): 15186–15192
23. Vispute R D, Talyansky V, Choopun S, Sharma R P, Venkatesan T, He M, Tang X, Halpern J B, Spencer M G, Li Y X, Salamanca-Riba L G, Iliadis A A, Jones K A. Heteroepitaxy of ZnO on GaN and its implications for fabrication of hybrid optoelectronic devices. Applied Physics Letters, 1998, 73(3): 348
24. Huang S Y, Yang J R. A Transmission electron microscopy observation of dislocations in GaN grown on (0001) sapphire by metal organic chemical vapor deposition. Japanese Journal of Applied Physics, 2008, 47(10): 7998–8002
25. Morin S A, Jin S. Screw dislocation-driven epitaxial solution growth of ZnO nanowires seeded by dislocations in GaN substrates. Nano Letters, 2010, 10(9): 3459–3463
26. Ozgur U, Alivov Ya I, Liu C, Teke A, Reshchikov M A, Dogan S, Avrutin V, Cho S J, Morkoc H J. A comprehensive review of ZnO materials and devices. Journal of Applied Physics, 2005, 98(4): 041301
27. Huang M H, Mao S, Feick H, Yan H, Wu Y, Kind H, Weber E, Russo R, Yang P. Room-temperature ultraviolet nanowire nano-lasers. Science, 2001, 292(5523): 1897–1899
28. Zhang J, Sun L D, Liao C S, Yang C H. A simple route towards tubular ZnO. Chemical Communications (Cambridge), 2002, 3(3): 262–263
29. Li Z Q, Xiong Y J, Xie Y. Selected-control synthesis of ZnO nanowires and nanorods via a PEG-assisted route. Inorganic Chemistry, 2003, 42(24): 8105–8109
30. Chen S J, Liu Y C, Shao C L, Mu R, Lu Y M, Zhang J Y, Shen D Z, Fan X W. Structural and optical properties of uniform ZnO nanosheets. Advanced Materials, 2005, 17(5): 586–590
31. Zeng H, Duan G T, Li Y, Yang S K, Xu X X, Cai W P. Blue luminescence of ZnO nanoparticles based on non-equilibrium processes: defect origins and emission controls. Advanced Functional Materials, 2010, 20(4): 561–572